Some analyses of potential profiles of forwardbiased highlow junctions

S. S. De and A. K. Ghosh

Citation: Journal of Applied Physics **75**, 2496 (1994); doi: 10.1063/1.357022
View online: http://dx.doi.org/10.1063/1.357022
View Table of Contents: http://scitation.aip.org/content/aip/journal/jap/75/5?ver=pdfcov
Published by the AIP Publishing

Some analyses of potential profiles of forward-biased high-low junctions

S. S. De and A. K. Ghosh
Centre of Advanced Study in Radio Physics and Electronics, University of Calcutta, 1 Girish Vidyaratna Lane, Calcutta-700 009, India

(Received 2 March 1993; accepted for publication 20 October 1993)

A model calculation for the variation of the normalized potential against the normalized position for a forward-biased, below 2 thermal voltage, high-low junction has been made through numerical computations of Poisson's equation. The model is oriented to a junction with a sufficiently large doping difference between the two sides.

I. INTRODUCTION

Poisson's equation with the use of Boltzmann statistics is a popular mathematical technique to study potential profiles in the surface region of a semiconductor step-junction and high-low junction.[1–3] The method usually yields an approximate relationship among normalized position, potential, and normalized field.

An alternative model for a high-low junction under the forward- biased condition, with a sufficiently large doping difference between the two sides, will be presented in this article to secure a new solution of Poisson's equation. It is assumed that across the n^+-n space charge region, a quasiequilibrium condition exists.[4] The condition of charge neutrality at the edges of the boundary will also be assumed to be maintained under the same condition.[5] For an abrupt n^+-n junction with low level injection in the n region, it can be seen that[4]

$$p_L(x)N_{DL}=p_R(x)N_{DR}.$$

It has been pointed out by Gunn[6] that the space charge region of a high-low junction consists of two distinctly different regions, viz., a depletion region on the heavily doped side and an accumulation region on the lightly doped side. Further, the potential difference across the depletion region is never greater than KT/q. Therefore the total normalized potential difference, which is the difference between the normalized bulk potential and the normalized junction potential, can never have a value greater than unity.[6,7] For this reason, the present model is utilized to study the potential profile in the highly doped side, i.e., the depletion region, controlled by the applied voltage and the total normalized potential difference (<1). In the lightly doped side, i.e., the accumulation region, the analyses are made for higher values of total normalized potential difference under biasing conditions.

Conventional analyses, similar to modeling of semiconductor step junctions and high-low junctions, are being carried out to show the variation of normalized potential with normalized position by choosing arbitrary values of different parameters that occur in the derivation of the solution of the Poisson equation. This has been compared with a previous work.[8]

To investigate the connection of this analysis to physical reality, the expression for effective surface recombination velocity is deduced on the basis of the present model (Appendix A). The variation of effective surface recombination velocity with the variation of dopant density is studied, the graphical presentation of which has been compared with earlier works.[9,10]

II. SITUATION UNDER FORWARD-BIASED HIGH-LOW JUNCTION

Poisson's equation of a high-low junction in equilibrium, where the left side is a highly doped n-type semiconductor, may be written as

$$\frac{d^2\phi}{dx^2}=-\frac{q}{\epsilon}(N_D-n), \tag{1}$$

where

$$n=n_i \exp U,$$

$$U=q\phi/KT=(E_F-E_i)/KT,$$

ϕ is the electrostatic potential, E_i is the Fermi level energy in the intrinsic semiconductor, E_F is the Fermi level energy, N_D is the ionized donor density, n_i is the density of holes and of electrons in the intrinsic semiconductor, and ϵ is the electrical permittivity.

Here, the effect of holes has been ignored and the donors are assumed to be completely ionized. The other symbols have their usual significance. The sketch of a n^+-n junction along with its band structure is shown in (a) and (b) of Fig. 1.

Poisson's equation for the left side is given by

$$\frac{d^2U_L}{dx^2}=-\frac{q^2}{\epsilon KT}[n_i\exp(U_{BL})-n_i\exp(U_L)], \tag{2}$$

where U_L and U_{BL} are the normalized potential at an arbitrary point on the left side and the normalized bulk potential at the left side, respectively.

When n_i is replaced by N_i, the nonequilibrium state of the semiconductor under the forward-biased condition would acquire virtually the state of an equilibrium semiconductor,[11] where

$$N_i=\left(\frac{N_{DL}^2+N_{DR}^2+2N_{DL}N_{DR}\cosh U_{HL}}{4\sinh^2 U_{HL}}\right)^{1/2}, \tag{3}$$

and U_{HL} is the normalized total potential difference across the transition region.

N_{DL} and N_{DR} are the donor densities at the left and right sides of the n^+-n junction as shown in Fig. 1. In

 0021-8979/94/75(5)/2496/6/$6.00

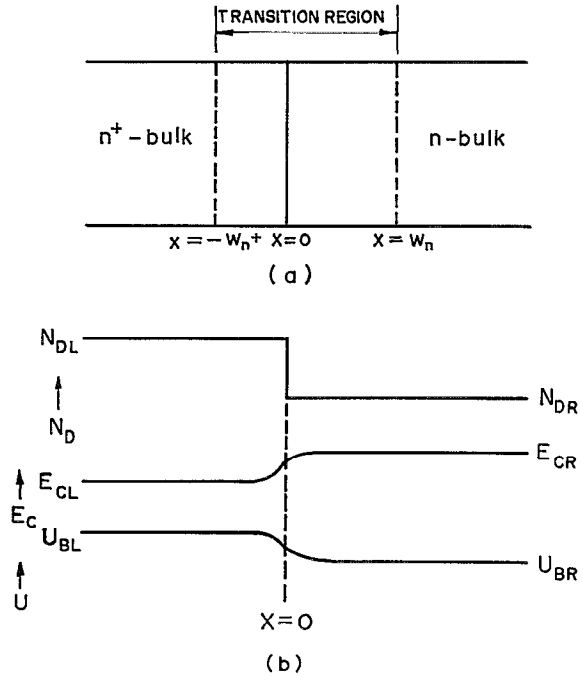

FIG. 1. Geometry and band diagrams of the stated high-low junction. (a) Referential coordinates for the n^+-n junction. (b) Variations of donor density, bottom of conduction band, and normalized potential U with distance normal to interface.

deducing the expression of N_i for the high-low junction with low injection in the n region, it is assumed that (i) the quasi-Fermi level is constant in the space charge region and (ii) the charge neutrality condition at the edges of the boundary is present.

The relationship between U_{HL} and applied biasing potential is given by

$$U_{HL}=U_A-\ln(N_{DL}/N_{DR}).$$

Here, the junction has been specified as

$$U'_{BL}=\ln(N_{DL}/N_i)$$

and the effective bulk potential before the onset of high-level condition is considered to be

$$U'_{BL}=U_{BL}-U_A/2.$$

The primes are used to distinguish the values of the quantities in biasing conditions from their nonbiasing situation.

Thus, Eq. (2) under biasing conditions becomes

$$\frac{d^2U_L}{dx^2}=-\frac{q^2}{\epsilon KT}[N_i\exp(U'_{BL})-N_i\exp(U'_L)]$$

$$=\frac{1}{2L_{Di}^2}[\exp(U'_L)-\exp(U'_{BL})], \tag{4}$$

where $L_{Di}=(\epsilon KT/2q^2N_i)^{1/2}$ is the intrinsic Debye length under biasing. Boundary conditions may be chosen as

$$U'_L\to U'_{BL} \quad \text{and} \quad \frac{dU'_L}{dx}\to 0 \quad \text{as} \quad x\to -W_{n+}.$$

Thus

$$\int_0^{\partial U/\partial x}\left(\frac{\partial U'_L}{\partial x}\right)d\left(\frac{\partial U'_L}{\partial x}\right)$$

$$=\frac{1}{2L_{Di}^2}\int_{U'_{BL}}^{U'_L}[\exp(U'_L)-\exp(U'_{BL})]dU'_L. \tag{5}$$

This yields

$$\left(\frac{dU'_L}{dx}\right)^2=\frac{1}{L_{Di}^2}[\exp(U'_L)-\exp(U'_{BL})$$

$$-(U'_L-U'_{BL})\exp(U'_{BL})]. \tag{6}$$

The boundary conditions for the right side may be stated as

$$U'_R\to U'_{BR} \quad \text{and} \quad \frac{dU'_R}{dx}\to 0 \text{ as } x\to W_n.$$

Here, U'_{BR} and U'_R are the normalized bulk potential and normalized potential at an arbitrary point on the right side, respectively. Poisson's equation will remain unchanged in form for this side also. Now,

$$\left(\frac{dU'_R}{dx}\right)^2=\frac{1}{L_{Di}^2}[\exp(U'_R)-\exp(U'_{BR})$$

$$-(U'_R-U'_{BR})\exp(U'_{BR})]. \tag{7}$$

This yields

$$\frac{x}{L_{Di}}=\int_{U'_J}^{U'_R}\frac{dU'_R}{[\exp(U'_R)-\exp(U'_{BR})-(U'_R-U'_{BR})\exp(U'_{BR})]^{1/2}}, \tag{8}$$

where U'_J is the normalized potential at the junction.

Since $L_{Di}=L_D(\cosh U'_{BR})^{1/2}$, the equation for the normalized position from (8) is given by

$$\frac{x}{L_D}=\frac{1}{\sqrt{2}}\int_{U'_J}^{U'_R}\left(\frac{\exp(U'_{BR})+\exp(-U'_{BR})}{\exp(U'_R)-\exp(U'_{BR})-(U'_R-U'_{BR})\exp(U'_{BR})}\right)^{1/2}dU'_R, \tag{9}$$

where L_D is the extrinsic Debye length under biasing, which is employed to reduce redundancy. In this presentation, all potentials in the n^+-n junction have been considered to be positive. Therefore, $U_{BL}>U_L>U_J>U_R>U_{BR}$. For brevity, as potential is decreasing in the positive x direction, different potentials in Eq. (9) can be transformed by the following relations:

$$U'_J-U'_{BR}\equiv W'_{JR} \quad \text{and} \quad U'_R-U'_{BR}\equiv W'_R,$$

where W'_{JR} is the effective normalized potential difference on the right side, and W'_R is the normalized potential difference between the remote end and an arbitrary point on the right side. These relations reveal that W'_R will also decrease with x, but it will have positive values:

$$W'_R=0 \quad \text{at} \quad x=W_n$$

and

$$W'_R=U'_{JR}-U'_{BR}=W'_{JR} \quad \text{at} \quad x=0.$$

Thus, for the accumulation region, Eq. (9) yields

$$\frac{x}{L_D}=-\frac{1}{\sqrt{2}}\int_{W'_R}^{W'_{JR}}\left(\frac{\exp(U'_{BR})+\exp(-U'_{BR})}{\exp(U'_{BR})[\exp(W'_R)-W'_R-1]}\right)^{1/2}\times dW'_R. \tag{10}$$

This becomes

$$\frac{x}{L_D}=-\frac{1}{\sqrt{2}}\int_{W'_R}^{W'_{JR}}\left(\frac{1+\exp(-2U'_{BR})}{\exp(W'_R)-W'_R-1}\right)^{1/2} dW'_R. \tag{11}$$

For the depletion region, in the left side, the transformation relation is chosen as $U'_{BL}-U'_J\equiv W'_{JL}$ and $U'_{BL}-U'_L\equiv W'_L$, where W'_{JL} and W'_L are the effective normalized potential difference on the left side, and the normalized potential difference between the remote end and an arbitrary point in the left side, respectively. Thus, for the depletion region, the expression for the normalized position becomes

$$\frac{x}{L_D}=\frac{1}{\sqrt{2}}\int_{W'_L}^{W'_{JL}}\left(\frac{1+\exp(-2U'_{BL})}{\exp(-W'_L)+W'_L-1}\right)^{1/2} dW'_L. \tag{12}$$

III. ANALYSIS AND DISCUSSION

As routine analyses, which are generally followed in device modeling or step-junction problems, an attempt has been made to study the variation of normalized potential under biasing (W') with normalized position (x/L_D) by choosing certain arbitrary values of different parameters.

Normalized bulk potential under biasing (U'_B) is an explicit function of applied voltage through N_i. It must change due to biasing. But the normalized bulk potential (U_B) does not change with biasing. For an arbitrarily chosen fixed value of U_B and applied voltage U_A, the value of U'_B may be considered as fixed. Under this circumstance, variations of normalized potential versus normalized position may be studied. As a result, the graphs in Figs. 2–4 are drawn based on numerical computation of Eqs. (11) and (12) for the depletion and accumulation regions, respectively. In this attempt, since the total potential drop on the left side, i.e., heavily doped side, is less than unity, in Fig. 2 the variation of normalized potential with position are studied in the depletion region for lower values of W'_{JL} (=0.3, 0.5, 0.7, 1.0). Here, the applied biasing $U_A=2$ thermal voltage and normalized bulk potential $U_{BL}=23$

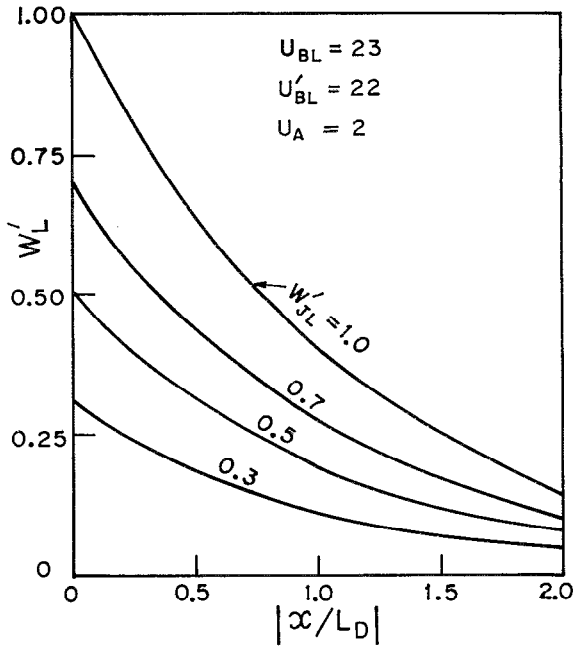

FIG. 2. Plots of normalized potential versus normalized position at the depletion region under biasing condition for different values of W'_{JL} (0.3,0.5,0.7,1.0), keeping $U'_{BL}=22$ in each case.

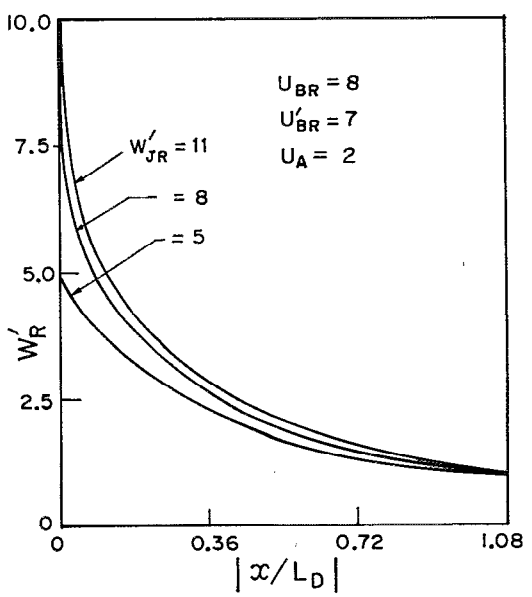

FIG. 3. Plots of normalized potential versus normalized position at the accumulation region under biasing conditions for different values of W'_{JR} (=5,8,11), keeping $U_{BR}=8$ in each case.

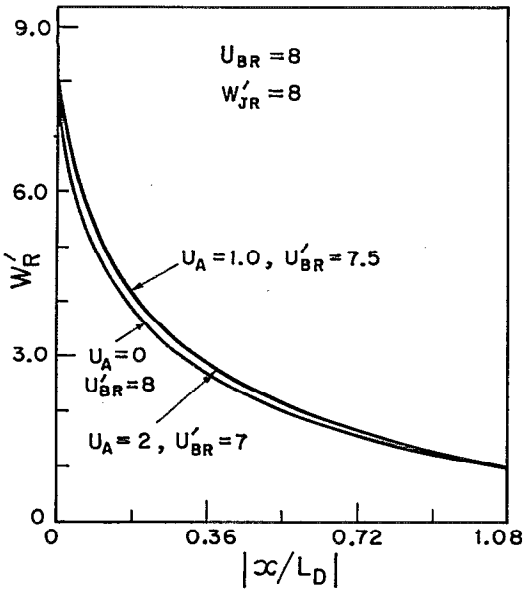

FIG. 4. Variation of normalized potential with normalized position in the accumulation region with different values of U'_{BR} and applied biasing thermal voltage U_A, for fixed values of U_{BR} and W'_{JR}.

are chosen arbitrarily. From the relation, it reveals that identical graphs will be obtained when $U_A=0$ for some other values of bulk potential. Obviously, the bulk potential under biasing condition changes. Therefore, the magnitude of normalized potential with normalized position will be different for different values of bulk potential under biasing. Though the junction is at $x=0$, the depletion region should be along the negative direction of the x axis.

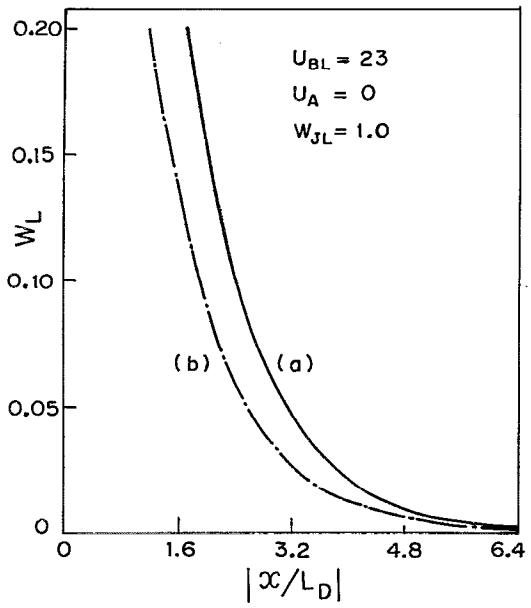

FIG. 5. Plots of normalized potential vs normalized position at the depletion region for $U_A=0$ and $W'_{JL}=W_{JL}=1.0$, keeping $U_{BL}=23$. The graph (a) depicts the results of the present analysis, while graph (b), indicated by the thin dashed line, is due to numerical computation made from the work of Missous and Rhoderick (Ref. 8).

But according to the transformation relations and as depicted in Fig. 2, the depletion sets may be taken along the positive direction of the x axis.

Figure 3 shows the variation of normalized potential with normalized position under biasing condition in the accumulation region for higher values of W'_{JR} $(=5,8,11)$ with an arbitrarily chosen value of applied biasing $U_A=2$ thermal voltage. In Fig. 4, a set of graphs are drawn for the given values of $U_{BR}=8$ and $W'_{JR}=8$. The graphs almost overlap for some chosen values of biasing and U'_{BR}. Thus it reveals that the value of U'_{BR} changes due to biasing. For some different values of applied voltage and the values of U'_{BR}, potential versus position curves yield nearly identical nature of variation.

The present work has been compared in Fig. 5 with a previous work[8] to study the variation of normalized potential with normalized position at the depletion region under identical conditions, i.e., unbiased conditions. The curve (a) represents the results of the present analysis for $U_A=0$ and $W'_{JL}=W_{JL}=1.0$, keeping $U_{BL}=23$, while the graph (b), indicated by the thin dashed line is the result of numerical computation of the earlier work.[8]

To investigate the physical reality of this analysis, an expression for effective surface recombination velocity has been deduced (Appendix A) on the basis of the present model by incorporating the influences of (i) the built-in field at the n^+-n junction, (ii) the minority carrier recombination in the n^+ region, and (iii) minority carrier recombination in the space charge layer at the n^+-n junction. These are not fully considered in the works of earlier authors.[9,12–14] The expression is given by (see Appendix)

$$S_{\text{eff}}=\frac{N_{DR}}{N_{DL}}\frac{D_{pn^+}}{L_{pn^+}}\coth\left(\frac{W_{n^+}}{L_{pn^+}}\right)+\frac{p_1}{N_{DL}}\frac{D_{pn^+}}{L_{pn^+}}\coth\left(\frac{W_{n^+}}{L_{pn^+}}\right)+\frac{\pi}{4q\tau_{pa}}\left(\frac{2KT\epsilon_{sn}}{N_{DL}\exp[q(\phi_n-\phi_b)/KT]}\right)^{1/2}+\frac{1.46}{q\tau_{pd}}\exp[q(\phi_n-\phi_b)/KT]\left(\frac{2KT\epsilon_{sn^+}}{N_{DL}}\right)^{1/2}. \quad \text{(A10)}$$

The first two terms on the right hand side of Eq. (A10) are the contribution to S_{eff} in the n^+ region. The first term corresponds to the result of earlier works,[9,12] arising only due to the minority carrier recombination in the n^+ region. The second term occurs due to the hole concentration in front of the n^+-n region, which is negligible in the n-base region at lightly doped conditions. The last two terms together represent the total contribution of the minority carrier recombination to S_{eff} in the space charge layer. The third and fourth terms arise out of recombination of holes in the accumulation and depletion layers, respectively. When the contribution of the influence stated in (iii) is neglected, Eq. (A10) will reduce to Eq. (22) of the earlier work[9] or to Eq. (12) of the earlier work.[12] Thus, a comparison between the earlier work[9] and the present work can be made taking into consideration only the first term of Eq. (A10). From this perspective, in Fig. 6, a plot of effective surface recombination velocity S_{eff} versus impurity concentration in the heavily doped side N_{DL} is drawn for some

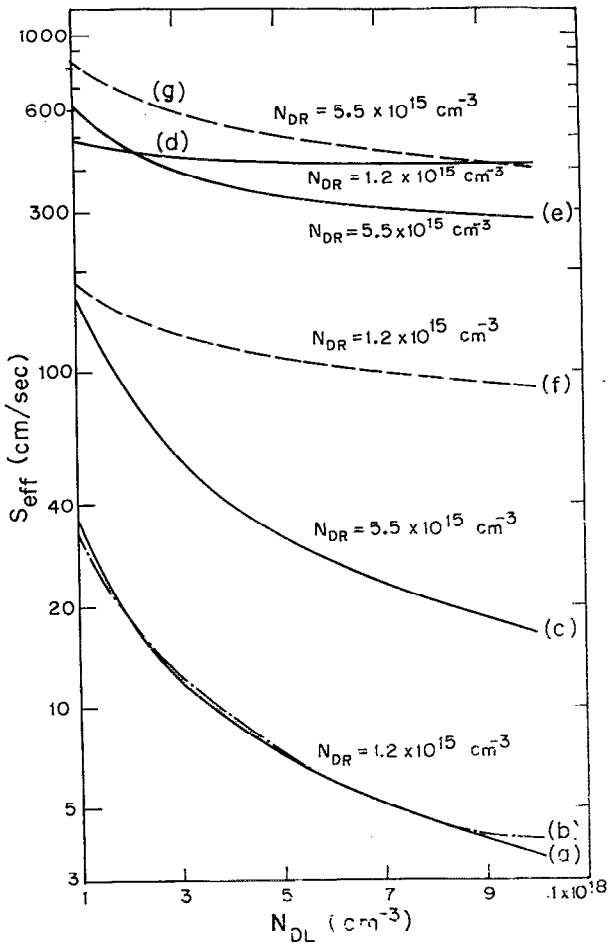

FIG. 6. Plots of S_{eff} vs N_{DL} for different values of N_{DR}. The solid line (a) represents the results of the present analysis, taking only the first term of the right hand side of Eq. (A10), whereas the results of Ram and Tyagi are shown by the thin dashed line (b). (c) is drawn similar to (a) but with some other value of N_{DR}. (d) and (e) are the results of complete computational analysis of Eq. (A10) for two different values of N_{DR}. The graphs (f) and (g), represented by the dotted lines, depict the results of an earlier work (Ref. 10) for $N_{DR}=1.2\times10^{15}$ cm^{-3} and 5.5×10^{15} cm^{-3}, respectively.

fixed values of impurity concentration of the lightly doped side N_{DR}. As such, the continuous graph [Fig. 6(a)] is obtained as a result of numerical computation of Eq. (A10), taking only its first term from the right hand side. The thin dashed line [Fig. 6(b)] indicates the earlier work.[9] This shows good agreement. Similarly, for a higher value of N_{DR}, the graph (c) is plotted depicting greater dependence of S_{eff} on N_{DR}. The values of N_{DR} are 1.2×10^{15} cm^{-3} for graphs (a) and (b) and 5.5×10^{15} cm^{-3} for graph (c), respectively. Curves (d) and (e) are drawn from the complete computational analysis of Eq. (A10). In (d), the values of N_{DR} are the same as chosen in (a) and (b), whereas for (e) it is the same as in (c). The graphs shown in Figs. 6(f) and 6(g), marked by dotted lines, depict the results from a previous work[10] for $N_{DR}=1.2\times10^{15}$ cm^{-3} and 5.5×10^{15} cm^{-3}, respectively. It reveals that at higher values of impurity concentration of the lightly doped side (N_{DR}), the previous work[10] approaches the results of complete computational analysis of the present work. But for relatively lower values of N_{DR}, the two results deviate considerably from each other. Thus, N_{DR} has a varying control over the variation of S_{eff} with N_{DL}.

APPENDIX A: EFFECTIVE SURFACE RECOMBINATION VELOCITY FOR THE n^+-n JUNCTION

For a high-low (n^+-n) junction, the space charge region has an accumulation layer on the n side, and a depletion layer on the n^+ side. The Poisson equations for both the accumulation and depletion regions may be written as

$$\frac{d^2\phi}{dx^2}=\frac{q}{\epsilon_{sn}}(N_{DR}-n),$$
$$\frac{d^2\phi}{dx^2}=-\frac{q}{\epsilon_{sn+}}(N_{DL}-n), \tag{A1}$$

where $\phi(x)$ is the potential in the space charge region, and N_{DL} (N_{DR}) is the impurity donor concentration in the $n^+(n)$ regions. The electron concentration $n(x)$ for the stated two regions is given by

$$n(x)=N_{DR}\exp\left[-\frac{q}{KT}(\phi_n-\phi)\right],$$
$$n(x)=N_{DL}\exp\left[\frac{q}{KT}(\phi_b-\phi_n+\phi)\right], \tag{A2}$$

where ϕ_b is the built-in potential barrier, and ϕ_n is the forward voltage drop across the n^+-n junction. Choosing the junction to be at $x=0$ and the space charge region edges at $X=-W_{n+}$ and W_n (Fig. 1), the following boundary conditions may be considered:

$$\phi(x)=0 \quad \text{at } x=W_n,$$
$$\phi(x)=-(\phi_b-\phi_n) \quad \text{at } x=-W_{n+},$$
$$\phi(x)=-\phi_0 \quad \text{at } x=0,$$
$$E=-\frac{d\phi}{dx} \quad \text{at } x=W_n,$$
$$E=0 \quad \text{at } x=-W_{n+},$$
$$E=E_0 \quad \text{at } x=0.$$

The expression of electric field E has been derived from Eq. (A1). For both the regions, these are given by

$$E=\mp\left(\frac{2qN_{DR}}{\epsilon_{sn}}\left\{-\phi+\frac{KT}{q}\times\exp\left(-\frac{q\phi_n}{KT}\right)\left[\exp\left(\frac{q\phi}{KT}\right)-1\right]\right\}\right)^{1/2},$$

$$E=\mp\left(-\frac{2qN_{DL}}{\epsilon_{sn^+}}\left\{(\phi_b-\phi_n+\phi)-\frac{KT}{q}\left[\exp\left(\frac{q(\phi_b-\phi_n+\phi)}{KT}\right)-1\right]\right\}\right)^{1/2}. \quad \text{(A3)}$$

The expression of recombination current density can be derived from the following current continuity equation for holes in the space charge layer of a forward biased high-low (n^+-n) junction as

$$\frac{1}{q}\frac{dJ_p}{dx}=\frac{p(x)}{\tau_{p0}}, \quad \text{(A4)}$$

where τ_{p0} is the effective minority carrier life time in the space charge region and $p(x)=p_1\exp(-q\phi/KT)$, where p_1 is the hole concentration at W_n. Thus, Eqs. (A3) yield the recombination current density J_r as

$$J_r=\frac{qp_1}{\tau_{p0}}\int\frac{\exp(-q\phi/KT)}{d\phi/dx}\,d\phi. \quad \text{(A5)}$$

Using the assumed boundary conditions in Eq. (A5) for the accumulation region and substituting the value of $d\phi/dx$ from Eqs. (A3) into Eq. (A5) along with the condition $\phi\ll(KT/q)\exp(-q\phi_n/KT)$ $[\exp(q\phi/KT)-1]$, one obtains the expression for recombination current density in the accumulation region as

$$J_{rac}=-\frac{qp_1}{\tau_{pa}}\left(\frac{2KT\epsilon_{sn}}{q^2N_{DR}\exp(-q\phi_n/KT)}\right)^{1/2}\pi/4, \quad \text{(A6)}$$

where τ_{pa} is the minority carrier life time in the accumulation region. Similarly, the expression for recombination current density in the depletion region may be obtained by using appropriate boundary conditions in Eq. (A5) and substituting the value of $d\phi/dx$ from Eqs. (A3) into Eq. (A5) with $\exp[q(\phi_b-\phi_n+\phi)/KT-1]\cong 0$. It is given by

$$J_{rdp}=\frac{qp_1}{\tau_{pd}}\frac{1.46(N_{DR}+p_1)}{N_{DL}}\left(\frac{2KT\epsilon_{sn^+}}{q^2N_{DL}}\right)^{1/2}, \quad \text{(A7)}$$

where τ_{pd} is the minority carrier life time in the depletion region. Thus, the total space charge recombination current density

$$J_{rsn}=J_{rac}+J_{rdp}.$$

At the farthest end of the depletion region, the hole recombination current density owing to the minority carrier recombination in the specified region may be obtained as

$$J_{prn^+}=-\frac{qD_{pn^+}}{L_{pn^+}}(p_2-p_{n^+})\coth\left(\frac{W_{n^+}}{L_{pn^+}}\right), \quad \text{(A8)}$$

where D_{pn^+} and L_{pn^+} are the diffusion coefficient and the diffusion length of holes, respectively, in the n^+ region. p_{n^+} is the hole concentration at the n^+ region. p_2 is the hole concentration at $-W_{n^+}$, and W_{n^+} is the thickness of the n^+ region. Total minority carrier recombination current density, when p_n is the hole concentration at the other extreme end of the accumulation region, is given by

$$J_{prn}=-qS_{\text{eff}}(p_1-p_n)=J_{rsn}+J_{prn^+}. \quad \text{(A9)}$$

The combination of Eqs. (A6)–(A9) with $p_2=(N_{DR}+p_1)p_1/N_{DL}$ and assuming $p_2\gg p_{n^+}, p_1\gg p_n$, one obtains the effective surface recombination velocity S_{eff} as

$$S_{\text{eff}}=\frac{N_{DR}}{N_{DL}}\frac{D_{pn^+}}{L_{pn^+}}\coth\left(\frac{W_{n^+}}{L_{pn^+}}\right)+\frac{p_1}{N_{DL}}\frac{D_{pn^+}}{L_{pn^+}}\coth\left(\frac{W_{n^+}}{L_{pn^+}}\right)+\frac{\pi}{4q\tau_{pa}}\left(\frac{2KT\epsilon_{sn}}{N_{DL}\exp[q(\phi_n-\phi_b)/KT]}\right)^{1/2}+\frac{1.46}{q\tau_{pd}}\exp[q(\phi_n-\phi_b)/KT]\left(\frac{2KT\epsilon_{sn^+}}{N_{DL}}\right)^{1/2}. \quad \text{(A10)}$$

[1] W. C. Johnson and P. T. Panousis, IEEE Trans. Electron. Devices **ED-18**, 965 (1971).
[2] S. N. Singh and P. K. Singh, Solid-State Electron. **33**, 968 (1990).
[3] S. S. De and A. K. Ghosh, Solid-State Electron. **32**, 517 (1989).
[4] R. W. Dutton and R. J. Whittier, IEEE Trans. Electron. Devices **ED-16**, 458 (1969).
[5] C. Y. Wu, Solid-State Electron. **23**, 641 (1980).
[6] C. G. B. Garrett and W. H. Brattain, Phys. Rev. **99**, 376 (1955).
[7] J. B. Gunn, J. Electron. Control **4**, 17 (1958).
[8] M. Missous and E. H. Rhoderick, Solid-State Electron. **28**, 233 (1985).
[9] G. V. Ram and M. S. Tyagi, Solid-State Electron. **24**, 753 (1981).
[10] C. Y. Wu, Solid-State Electron. **23**, 641 (1980).
[11] H. Guckel, D. C. Thomas, S. V. Iyengar, and A. Demirkol, Solid-State Electron. **20**, 647 (1977).
[12] J. del Alamo, J. Van Meerbergen, F. d'Hoore, and J. Nijs, Solid-State Electron. **24**, 533 (1981).
[13] S. N. Singh and G. C. Jain, Sol. Cells **5**, 143 (1982).
[14] B. H. Rose, IEEE Trans. Electron. Devices **ED-31**, 559 (1984).